Developmental Cell, Vol. 8, 949–961, June, 2005, Copyright ©2005 by Elsevier Inc. DOI 10.1016/j.devcel.2005.03.018

Absence of Mouse REC8 Cohesin Promotes Synapsis of Sister Chromatids in Meiosis

Huiling Xu,[1,3] Matthew D. Beasley,[1,3] William D. Warren,[1,4,5] Gijsbertus T.J. van der Horst,[2,4] and Michael J. McKay[1,*]

[1]Divisions of Radiation Oncology and Research
Peter MacCallum Cancer Centre
Melbourne, Victoria 8006
Australia

[2]Department of Cell Biology and Genetics
Center for Biomedical Genetics
Erasmus University Rotterdam
3000 DR Rotterdam
The Netherlands

Summary

REC8 is a key component of the meiotic cohesin complex. During meiosis, cohesin is required for the establishment and maintenance of sister-chromatid cohesion, for the formation of the synaptonemal complex, and for recombination between homologous chromosomes. We show that REC8 has an essential role in mammalian meiosis, in that *Rec8* null mice of both sexes have germ cell failure and are sterile. In the absence of REC8, early chromosome pairing events appear normal, but synapsis occurs in a novel fashion: between sister chromatids. This implies that a major role for REC8 in mammalian meiosis is to limit synapsis to between homologous chromosomes. In all other eukaryotic species studied to date, REC8 phenotypes have been restricted to meiosis. Unexpectedly, *Rec8* null mice are born in sub-Mendelian frequencies and fail to thrive. These findings illuminate hitherto unknown REC8 functions in chromosome dynamics during mammalian meiosis and possibly in somatic development.

Introduction

Meiosis is a highly specialized program of eukaryotic cell division that generates genetically diverse haploid gametes. During prophase of meiosis I, replicated sister chromatids search for, align, and pair with their homologous partner. Recombination then occurs between paired homologous chromosomes, which establishes a physical link between homologs that facilitates their segregation during the first meiotic division. Meiotic recombination is associated with the formation of the synaptonemal complex (SC), a meiosis-specific proteinaceous structure that binds homologous chromosomes together in a process termed synapsis. The SC, which is thought to function in facilitating and coordinating genetic recombination, dissolves at the end of prophase I. Resolution of the resulting chiasma-linked chromosome pairs requires temporally and spatially regulated loss of cohesion between sister chromatids.

Sister-chromatid cohesion (SCC) is established during replication of both mitotic and meiotic chromosomes by a multiprotein complex called "cohesin." During meiosis, loss of chromosome arm cohesion from sister chromatids, but not centromeres, at anaphase I permits homologous chromosomes to separate by a "reductional" meiotic division. Sister chromatids remain attached at their centromeres until the second meiotic division. At the transition of metaphase II and anaphase II, the loss of centromeric cohesion between sister chromatids allows the segregation of individual sister chromosomes to each haploid gamete by "equational" division. SCC may also have additional roles in ensuring "biorientation," which guides the attachment of sister kinetochores to microtubules emanating from opposite spindle poles (Nasmyth, 2001).

The core eukaryotic mitotic cohesin complex consists of four proteins: two structural-maintenance-of-chromosomes (SMC) proteins, SMC1 and SMC3, and two non-SMC subunits, RAD21/SCC1/MCD1 and SCC3 (Guacci et al., 1997; Michaelis et al., 1997). SMC1 and SMC3 form a heterodimer and provide the structural backbone of the cohesin complex (Jessberger, 2002). RAD21/SCC1 binds to SMC head domains via its terminal conserved domains and SCC3 associates with the complex though RAD21/SCC1 (Haering et al., 2002). Other associated proteins (e.g., SCC2, PDS5, TIM-1) assist in SCC, in both mammals and in other species (Chan et al., 2003; Ciosk et al., 2000; Hartman et al., 2000).

During meiosis, the RAD21/SCC1 cohesin subunit is replaced by a meiotic-specific isoform, called REC8, in both budding yeast (*Saccharomyces cerevisiae*) and fission yeast (*Schizosaccharomyces pombe*) (Klein et al., 1999; Molnar et al., 1995). Fission yeast also has two paralogs of Scc3: psc3+ and rec11+ (Kitajima et al., 2003). Deletion of the *Rec8* gene in either yeast species produces a number of meiotic dysfunctions, including failures of SC formation, chromosome cohesion, and meiotic recombination (Klein et al., 1999; Molnar et al., 1995; Watanabe and Nurse, 1999). Thus, REC8 and the eukaryotic meiotic cohesin complex are key participants in the cellular programs unique to meiotic division.

Depletion of REC8 by RNA interference (RNAi) in *Caenorrhabditis elegans* (Pasierbek et al., 2001) resulted in defects in recombination, SC formation, and cohesion, similar to those of the yeast mutants. Mammalian *Rec8* orthologs have been identified (McKay et al., 1996; Parisi et al., 1999). Their chromosome distribution in germ cells support their role as meiotic cohesins (Eijpe et al., 2003; Lee et al., 2003). However, studies of mammalian meiotic cohesins revealed that there exist a number of differences from other species (Jessberger, 2002). For instance, vertebrates have a greater degree of complexity in the number of components of

*Correspondence: michael.mckay@petermac.org
[3]These authors contributed equally to this work.
[4]These authors contributed equally to this work.
[5]Present address: Comparative Genomics Centre, James Cook University, Townsville, Queensland 4811, Australia.

both the mitotic and meiotic cohesin complexes (Jessberger, 2002). This raises the question as to how these meiotic cohesin subunits associate and function in mammalian meiosis.

A very recent report described a mutant *Rec8* allele from a genome-wide mutagenesis screen in mice (Bannister et al., 2004). Mutant mice (*mei8*) carried a nonsense *Rec8* mutation, which prematurely truncated REC8 at amino acid 154, potentially leaving at least one major functional domain intact. It is unknown whether this mutation results in a partial or complete phenotype. Homozygous mutants ($Rec8^{mei8}/Rec8^{mei8}$) of both sexes were sterile but were otherwise overtly normal. Chromosome spreads of male meiocytes showed that components of the SC and cohesin subunits STAG3 and SMC1α were loaded onto chromatid cores, but the status of female meiocytes was not reported.

We deleted all coding exons of the mouse *Rec8* gene by gene targeting (Beasley et al., 1999). Here, we report that abrogation of mouse *Rec8* gene function results in failure of mutant meiocytes to complete meiotic prophase I in both males and female *Rec8* mutant meiocytes. Most interestingly, we found that formation of synaptonemal complexes occurs between sister chromatids, rather than (as is the usual case) between homologous chromosomes, revealing an essential role for REC8 in proper SC topography. In addition to the meiotic blockage, and in contrast to *mei8* mutants, we found that *Rec8* null mutants exhibited a high incidence of embryonic lethality and a failure to thrive.

Results

Targeted Disruption of the *Rec8* Locus

The mouse *Rec8* locus comprises 20 exons spanning ~7 kb (see Supplemental Figure S1A available with this article online) and encodes a predicted protein of 591 amino acids that is highly homologous to the human REC8 protein (Parisi et al., 1999). RNA blot analysis showed *Rec8* mRNA to be highly abundant in mouse testis; however, a low level of *Rec8* mRNA was also detected during embryogenesis and in multiple somatic tissues, including thymus, lung, liver, kidney, and small intestine (data not shown). This result is consistent with multiple mouse tissue gene expression profiling by microarray analysis (http://symatlas.gnf.org/SymAtlas/).

To examine the consequences of abolition of *Rec8* function in mice, 19 coding exons of the *Rec8* locus were deleted by homologous recombination (Supplemental Figures S1A and S1B). Mice homozygous for the deleted allele did not express *Rec8* mRNA in the testis (Supplemental Figure S1C), indicating successful abolition of *Rec8* gene expression.

Mice Lacking *Rec8* Display a High Mortality Rate Both In Utero and Ex Utero, Germ Cell Failure, and Sterility

$Rec8^{-/-}$ pups were born from heterozygous parents at a frequency of only 12% (n = 1090, all genotypes), much lower than the 25% expected from Mendelian distribution ($p < 0.005$). The frequency of $Rec8^{-/-}$ embryos was approximately 16% (n = 94) at 13.5 days postcoitum (dpc), again lower than the expected Mendelian distribution, although not statistically significant ($p = 0.1$). $Rec8^{-/-}$ mice displayed both in utero and postnatal growth retardation compared to their wt and heterozygous littermates (Supplemental Figure S1D). The ratio of $Rec8^{-/-}$ male to female births was not significantly different (n = 1090 total: 60 males versus 71 females, $p = 0.3$). Macroscopic and histological examination of multiple deceased $Rec8^{-/-}$ animals failed to identify a common cause of death.

Rec8 null mice that survive to reach sexual maturity are sterile. Histological examination of $Rec8^{-/-}$ male epididymis revealed that sterility was due to a complete absence of mature sperm or their precursors (Figure 1A). Although a basal layer of spermatogonia was retained, some seminiferous tubules of $Rec8^{-/-}$ testis were almost depleted of primary spermatocytes by 19 days postpartum (dpp) (Supplemental Figure S2). Spermatids and spermatozoa were completely absent in adult $Rec8^{-/-}$ tubules (Figure 1B). TUNEL staining revealed that the prevalence of apoptotic cells in $Rec8^{-/-}$ testes tubules was significantly higher than wt testis (Figure 1C and Supplemental Figure S3). Both wt and $Rec8^{-/-}$ tubules have a basal layer of PCNA (a mitotic proliferation marker)-positive mitotic spermatogonial cells (Figure 1D), suggesting that mitotic proliferation was unaffected in $Rec8^{-/-}$ tubules, and consequently, the high levels of cell death are most likely responsible for the testis tubular defects causing the sterility of $Rec8^{-/-}$ males.

Axial Cores of $Rec8^{-/-}$ Spermatocytes Are Abnormal in Number and Appearance

Deletion of *Rec8* gene abrogates the formation of axial elements (AEs) and SC in budding yeast (Klein et al., 1999) or their equivalent structures in fission yeast (Molnar et al., 1995). RNAi-mediated REC8 depletion resulted in similar phenotypes in *C. elegans* (Pasierbek et al., 2001). To determine if this also pertained to mice, AEs (known as the lateral elements [LEs] of the SC following homolog synapsis) were examined by immunostaining using an antibody detecting the SCP3 component of AEs/LEs and also by silver staining of surface-spread spermatocyte chromosomes.

SCP3 marks the development of the AE and SC during meiotic prophase I (Dobson et al., 1994; Lammers et al., 1994). As previously reported in wt cells, a patchy deposition of SCP3 commences along univalent chromosomes (comprising cojoined sister chromatids) in leptonema (Dobson et al., 1994; Lammers et al., 1994). SCP3 accumulation extends along the full length of chromosomes as cells progress to zygonema where pairing and initiation of synapsis between homologous chromosomes is readily discernible (Figure 2A). With the completion of homolog synapsis in pachynema, 20 synapsed wt homologous chromosomes are fully connected by SCs (Figure 2B). In diplotene, homologs desynapse, but SCP3 remains along chromosome axes until the end of prophase I (Dobson et al., 1994).

Examination of $Rec8^{-/-}$ spermatocytes from adult testes by SCP3 staining revealed several types of meiotic prophase cells. Leptotene-like nuclei, with short stretches of fine-caliber SCP3, were observed, indicating that the chromosome core-associated SCP3 pro-

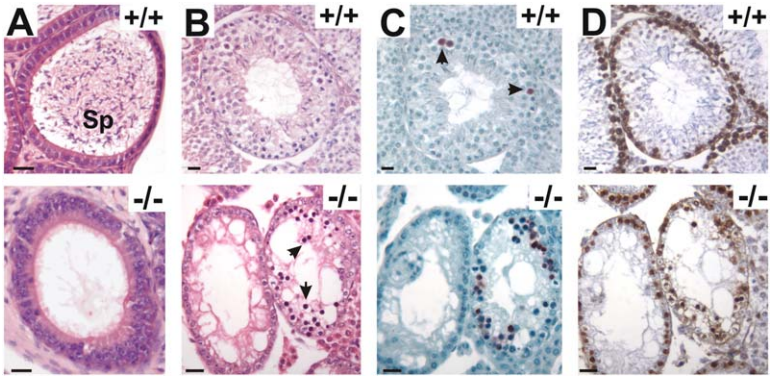

Figure 1. Spermatogenesis Failure in *Rec8*$^{-/-}$ Mutants

(A) Transverse hematoxylin and eosin (H&E)-stained sections of wt and *Rec8*$^{-/-}$ epididymis from adult males. Sp, spermatozoa.

(B) H&E sections of wt and *Rec8*$^{-/-}$ testes from adult males. Multiple, ordered germ cell layers are present in wt animals, while massive germ cell depletion occurs in *Rec8*-null animals. Arrows indicate deeply hematoxylin-staining pyknotic nuclei.

(C) Staining of serial testis sections for apoptosis by TUNEL assay. Wild-type tubules show occasional brown TUNEL-positive apoptotic cells (arrows). The *Rec8* null tubules had multiple TUNEL-positive cells.

(D) Proliferating cell nuclear antigen (PCNA)-stained, mitotically cycling spermatogonial cells in both wt and *Rec8*$^{-/-}$ testes.

Scale bars equal 20 μM.

tein was loaded in an apparently normal fashion during early meiotic prophase in *Rec8*$^{-/-}$ spermatocytes (data not shown). Nuclei with almost continuous SCP3 fibers were also observed, indicating that SCP3 deposition extended along at least most of the *Rec8*$^{-/-}$ chromosome cores (Figures 2C and 2D). However, typical pachytene nuclei with 20 synapsed chromosome cores were never observed in *Rec8*$^{-/-}$ mutant cells. Instead, approximately 40 SCP3-positive cores with a variety of chromosome appearances, likely to represent different stages of an aberrant *Rec8*$^{-/-}$ meiosis, were seen (Figures 2C–2E). A quantitation of the different *Rec8*$^{-/-}$ chromosome core morphologies is shown in Supplemental Table S2. In adult males, the two most frequent types of *Rec8*$^{-/-}$ zygotene-like nuclei were one that had most AEs lying in close proximity to a AE of similar length (Figure 2C), and another that had dispersed AEs (Figure 2D). Silver staining of spermatocyte chromosome spreads showed the similar chromosome appearance of approximately 40 axial cores in *Rec8*$^{-/-}$ zygotene-like spermatocytes, whereas this nuclear morphology was never observed in wt pachytene sper-

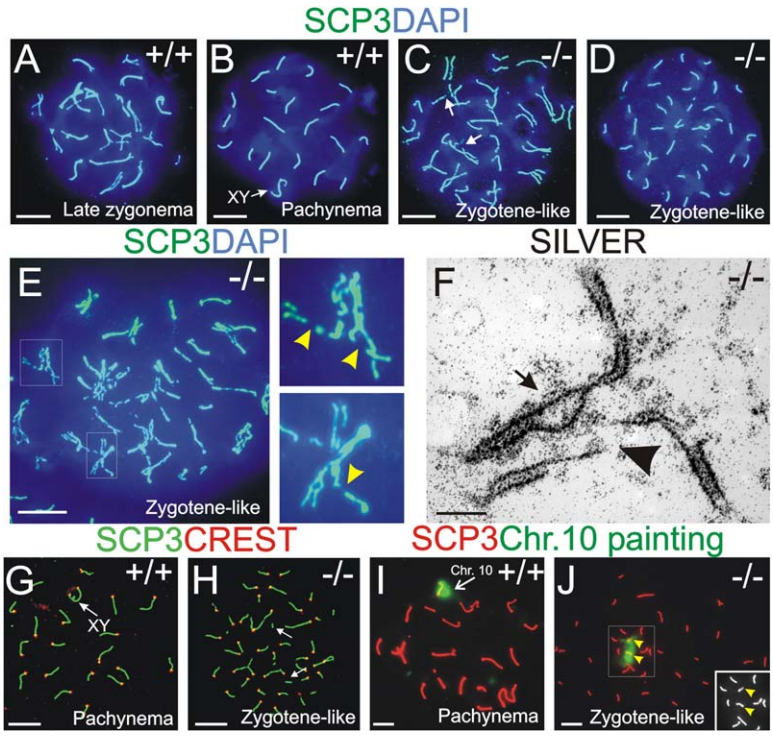

Figure 2. Failure of Homolog Synapsis in *Rec8*$^{-/-}$ Spermatocytes

(A and B) SCP3 staining (blue-green) of wt chromosomal axes at late zygonema (A) and pachynema (B) showing 20 synapsing chromosomes, including the XY sex chromosomes (arrow). Chromatin is counterstained with DAPI (blue).

(C and D) SCP3 staining of *Rec8*$^{-/-}$ zygotene-like spermatocyte spreads, showing two typical types of nuclei, one with a number of distantly paired chromosomes (C) and the other with dispersed chromosomes (D). For both nuclei, approximately 40 chromosome cores can be identified. Arrows indicate AE/LE gaps.

(E) *Rec8*$^{-/-}$ zygotene-like spermatocyte nucleus, with extensive chromosome fragmentation and widespread AE/LE bifurcation. Higher magnification of the boxed regions shows paired chromosomes, each with two strands of AE along the chromosome arms, in addition to sister-chromatid gaps (arrowheads).

(F) EM of silver-stained chromosomes, showing paired chromosomes with AE/LE fragmentation (arrowhead) and a region with apparently separated sister-chromosome axes (arrows).

(G and H) Costaining of chromosome cores (SCP3, green) and centromeres (CREST antisera, red) in wt (G) and *Rec8*$^{-/-}$ zygotene-like (H) spermatocytes. Arrows indicate chromosome fragments without CREST staining.

(I and J) Simultaneous chromosome 10 (green) painting and the SCP3 staining (red). Two AE/LEs (arrowheads) representing unsynapsed homologous chromosome 10 axes were embedded by the FISH signal in *Rec8*$^{-/-}$ nuclei (J). Insert shows a higher magnification of SCP3 staining alone (boxed), not to scale.

Scale bars equal 1 μM in (F) and 10 μM in all other panels.

matocytes (data not shown). These results strongly suggested that, unlike *Rec8* mutants in other eukaryotes, elimination of mouse *Rec8* function did not abolish AE/LE formation.

We observed occasional but clearly visible AE/LE discontinuities in the majority of *Rec8*$^{-/-}$ zygotene-like spermatocytes (Figure 2C, arrows). However, a subset of *Rec8*$^{-/-}$ zygotene-like spermatocytes had numerous breaks and bifurcations in their AE/LEs, as revealed by SCP3 immunostaining (Figure 2E). These cells constituted ~5% of prepubertal (16 dpp) spermatocytes and 13% of adult spermatocytes (Supplemental Table S2). The extent of AE breakage varied between nuclei. In some cases, AE/LEs were severely fragmented and split into two strands, presumably representing two sister-chromatid cores, along most of their length (Figure 2E). Further examination by EM confirmed the presence of gaps and apparent separation of individual AE/LEs in these *Rec8*$^{-/-}$ spermatocytes (Figure 2F).

Homologous Chromosome Synapsis Is Disrupted in *Rec8*$^{-/-}$ Meiocytes

An abnormal number of chromosomes could result from chromosome fragmentation, an extra round of DNA replication, or a failure in homologous chromosome synapsis. To distinguish among these possibilities, we performed further experiments. First, chromosome cores were coimmunostained with CREST antiserum in addition to SCP3. CREST signal, representing centromeres, was detected in the great majority of SCP3-positive chromosome cores (Figures 2G and 2H for wt and *Rec8*$^{-/-}$, respectively). This result suggests that chromosome fragmentation per se was unlikely responsible for the abnormal number of chromosome cores. Second, testicular cells (wt, *Rec8*$^{+/-}$, and *Rec8*$^{-/-}$) were disaggregated and analyzed for cell ploidy by flow cytometry to determine if an extra round of DNA replication might have occurred in premeiotic *Rec8*$^{-/-}$ primary spermatocytes. If this were the case, *Rec8*$^{-/-}$ primary spermatocytes would be expected to be octaploid (8N), rather than tetraploid (4N). No evidence of elevated numbers of 8N cells could be found in *Rec8*$^{-/-}$ testes as determined by flow cytometry (Supplemental Figure S4 and Supplemental Table S1). These results confirm that *Rec8*$^{-/-}$ spermatocytes do not contain a tetraploid complement of synapsed homologous chromosomes (bivalents).

Third, we performed fluorescence in situ hybridization (FISH) using a chromosome 10-specific paint probe in combination with SCP3 immunostaining. This technique allows the visualization of a specific chromosome and its axial core simultaneously. In wt pachytene spermatocytes, where homologous chromosomes are fully synapsed, a single SCP3-positive chromosome core was observed within the FISH signal, as expected (Figure 2I). In contrast, two distinct axial cores were associated with the chromosome 10 FISH signal in *Rec8*$^{-/-}$ spermatocytes (Figure 2J, and data not shown). These experiments demonstrated that the distantly paired chromosome axes in *Rec8*$^{-/-}$ spermatocytes represent homologous chromosomes (in this case, chromosome 10). Hence, failure of homologous chromosome synapsis is likely to be responsible for the abnormal number of chromosomes in *Rec8*$^{-/-}$ spermatocytes.

Sister-Chromatid Synapsis Occurs in *Rec8*$^{-/-}$ Meiocytes

To determine the extent of disruption of homolog synapsis in *Rec8*$^{-/-}$ spermatocytes, we conducted indirect immunofluorescence studies using an antibody to another integral SC protein, SCP1 (SYN1). SCP1 is a component of the transverse filament (TF), the structure that bridges the gap between two adjacent LEs during synapsis, and is a well-recognized marker for homolog synapsis. Colabeling of SCP1 and SCP3 highlights regions of synapsis in wt (Meuwissen et al., 1992). SCP1 is absent in leptonema and in early zygonema when homologous chromosomes start becoming aligned (Figure 3A). SCP1 localizes to sites of homolog synapsis in late zygotene, pachytene, and diplotene stages (Figures 3B–3E, respectively). In diplotene, the SCP1 signal is lost from desynapsed regions of homologous chromosomes (Figures 3D and 3E).

Colabeling of SCP1 with SCP3 on spreads of *Rec8*$^{-/-}$ spermatocytes revealed an unexpected variety of chromosome core appearances (Figures 3F–3I and Supplemental Table S2). At least six types of *Rec8*$^{-/-}$ spermatocytes could be distinguished, based on the patterns of SCP1 and SCP3 staining (Supplemental Table S2). Short stretches of SCP1 were evident in *Rec8*$^{-/-}$ leptotene-like (Supplemental Table S2) and zygotene-like (Figure 3F) type A spermatocytes. To our knowledge, the association of SCP1 with prezygotene chromosomes has not been previously observed in wt germ cells. In zygotene-like type B nuclei, where the majority of chromosomes are paired, discontinuous stretches of SCP1 staining were detected along pairs of chromosomes, although staining was not necessarily restricted to regions of close homolog association (Figure 3G). The extent of SCP1 binding also appeared to be heterogeneous within the each nucleus, ranging from short segments to more than half the length of some unpaired chromosomes (Figure 3G). We also noted that SCP1 was absent from some chromosomes, either entirely or for the most part of their length (Figure 3G, arrowheads). SCP1 binding was detected along the length of almost every univalent in zygotene-like type D (Figures 3H and 3I) and type E (Supplemental Table S2B) nuclei. Despite the extensive SCP1 binding, the majority of univalents in these *Rec8*$^{-/-}$ nuclei remained clearly separated (Figures 3H and 3I). Partly conjoined chromosome pairs, varied in numbers (1 to 11 pairs per cell) and positions, were observed in both type D and E nuclei (Figure 3I and Supplemental Table S2B). In such cases, SCP1 was present along both separated and conjoined regions (Figure 3I).

The presence of SCP1 on *Rec8*$^{-/-}$ univalents raised the possibility that an SC-like structure was being laid down between sister chromatids in *Rec8*$^{-/-}$ spermatocytes, rather than between homologous chromosomes as is the case in wt spermatocytes. To explore this possibility, we analyzed the ultrastructure of *Rec8*$^{-/-}$ spermatocyte chromosomes by EM. The distinctive tripartite structure of the mature SC, consisting of two LEs and a central element (CE), was readily discerned in wt pachytene cells (Figure 3J). AEs/LEs were also clearly evident in *Rec8*$^{-/-}$ spermatocytes. Notably, in *Rec8*$^{-/-}$ chromosomal regions where CEs were observed, the two LEs were separated by a distance similar to the LE

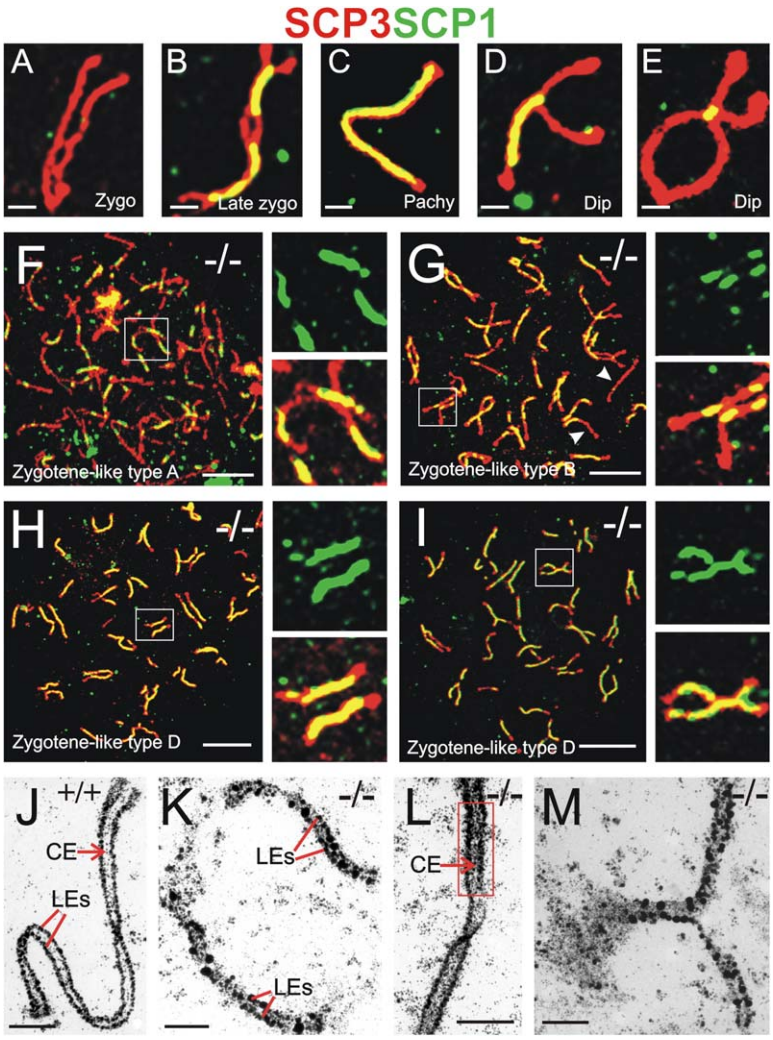

Figure 3. Synapsis Occurs between Sister Chromatids rather than between Homologs in *Rec8*$^{-/-}$ Spermatocytes

(A–E) Immunostaining of wt spermatocyte chromosome spreads for SCP3 (staining for axial elements, red) and SCP1 (staining for central elements, green); colocalization, yellow. Representative homolog pairs are shown from nuclei of zygonema (A), late zygonema (B), pachynema (C), and diplonema (D and E). Zygo, zygotene; Pachy, pachytene; Dip, diplotene.

(F–I) Immunostaining of *Rec8*$^{-/-}$ spermatocyte chromosome spreads for SCP3 (red) and SCP1 (green). Representative *Rec8*$^{-/-}$ nuclei showing patchy SCP1 staining on univalents (F); SCP1 binding at multiple sites along univalents (G); SCP1 staining along nearly the length of paired chromosomes (H), or along two partially conjoined chromosomes (I). Higher-power views show a selected region (boxed and to the right of main panel) for SCP1 staining alone (top) and overlay of SCP3 and SCP1 (bottom).

(J) Transmission EM of silver-stained wt pachytene chromosomes. Synapsed homologous chromosomes, showing the lateral elements (LEs, indicated) and a central element (CE, red arrow) of the SC.

(K–M) EM of representative *Rec8*$^{-/-}$ chromosomes.

(K) Paired *Rec8*$^{-/-}$ chromosomes, revealing two lateral elements (LEs) per univalent.

(L) A *Rec8*$^{-/-}$ univalent with a clearly visible central element (CE, red arrow and box). The intersister distance closely approximates the interhomolog distance in wt cells: compare with (J).

(M) Fork-like *Rec8*$^{-/-}$ chromosomes.

Scale bars equal 10 μM for (F)–(I) and 1 μM for all other panels.

separation between homologous chromosomes in wt cells (compare Figures 3J and 3L). Examination of partly conjoined fork-like *Rec8*$^{-/-}$ chromosomes revealed that two distinct LEs were present in the synapsed regions not only of univalents but also of bivalents (Figure 3M). There are a number of possibilities regarding the composition of such structures. First, short stretches of homologous synapsis can occur in some *Rec8*$^{-/-}$ nuclei (possibly dependent on non-*Rec8*-containing cohesin complex). Second, morphologically normal SC might form in the absence of sister-chromatid cohesion. Third, two nonsister chromatids might be involved in the homologous synapsis (-like) regions. Fourth, strand exchange may have occurred between synapsed sisters, with small regions of branch migration. We cannot presently distinguish among these possibilities.

The SCP1 immunostaining and EM observations strongly suggest that in the absence of REC8, a SC-like structure is assembled between sister-chromosome cores (i.e., sister synapsis), rather than between homologous chromosomes. It is unclear whether the formation of AE/LEs on the core of each sister chromatid in *Rec8*$^{-/-}$ spermatocytes is a direct or indirect consequence of the *Rec8* deletion. Splitting of the AE into two elements was also reported for a *Sordaria macrospora spo76-1* mutant (van Heemst et al., 1999). *Sordaria* SPO76 is related to budding yeast PDS5, an evolutionarily conserved gene that is essential for the maintenance of sister-chromatid cohesion (Hartman et al., 2000). Detailed ultrastructure studies of the wt murine SC indicated that the AE/LEs may be deposited along individual wt meiotic sister chromatids (Dietrich et al., 1992). Possibly, the proximity of paired sister chromatids normally renders these two AE/LE strands as a single functional unit and their dual nature is not usually evident in wt cells, but it is in *Rec8*$^{-/-}$ meiocytes and the *spo76-1* mutant where sister chromatids have lost their tight association.

Cohesins SMC3 and RAD21/SCC1 Are Present on *Rec8*$^{-/-}$ Chromosome Axes

REC8 is a core component of the multiprotein meiotic cohesin complex. We therefore investigated whether the chromosomal association of other cohesin subunits was perturbed in the absence of REC8. Consistent with

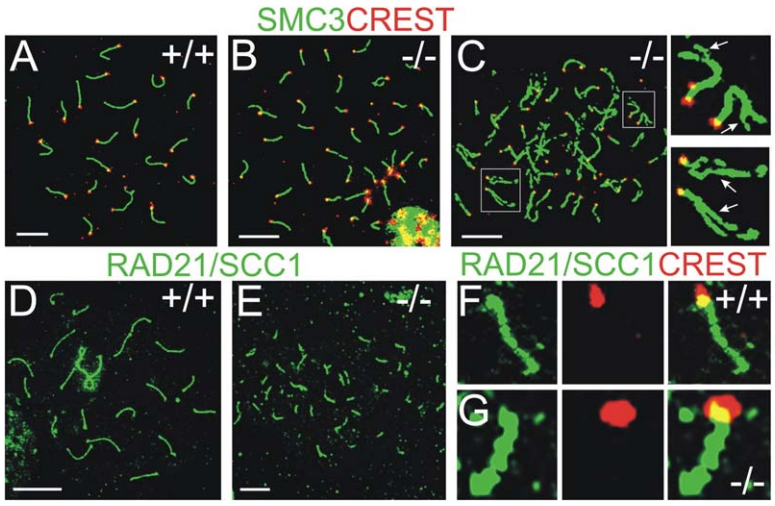

Figure 4. Localization of Cohesin Components on Meiotic Chromosome Cores

(A–C) Immunostaining for SMC3 cohesin (green) and centromeres (red). Colocalization: yellow. SMC3 staining decorates chromosome cores (green) and partially colocalizes with CREST on centromeres (yellow) in both wt pachytene (A) and *Rec8*$^{-/-}$ (B) spermatocyte spreads. (C) SMC3 staining was retained in regions of loss of sister-chromatid association (arrows). Inserts show higher-power views of selected chromosome pairs from (C) (boxed), not to scale.

(D–G) Immunostaining of spermatocyte chromosome spreads for RAD21/SCC1 cohesin (green) and centromeres (red). RAD21/SCC1 localizes contiguously along chromosome cores of wt pachytene (D) and *Rec8*$^{-/-}$ (E) spermatocytes. RAD21/SCC1 partially colocalizes with CREST at centromeres in wt (F) and *Rec8*$^{-/-}$ (G) chromosomes; not to scale. Scale bars equal 10 μM.

previous reports (Eijpe et al., 2000; Eijpe et al., 2003), SMC3 could be detected in wt spermatocytes from leptonema onward, and it localized essentially contiguously along the entirety of bivalents, including a part of the centromeres, in zygotene and pachytene nuclei (Figure 4A; data not shown). Patterns of SMC3 distribution in *Rec8*$^{-/-}$ leptotene spermatocytes were also as seen in wt cells (data not shown). In the majority of *Rec8*$^{-/-}$ zygotene-like spermatocytes, SMC3 was found contiguously along chromosome arms and on centromeres (Figure 4B). This observation is consistent with data from *C. elegans,* where RNAi-mediated deletion of REC8 or SCC3 cohesin subunits did not perturb SMC3 binding to chromosome cores (Chan et al., 2003). We noted that in *Rec8*$^{-/-}$ zygotene-like type C spermatocytes (Supplemental Table S2), part of the univalent chromosome arms was visualized as two individual chromosome axes by SMC3 staining (Figure 4C). This axial bifurcation, which was also observed with SCP3 and silver-stained preparations (Figures 2E and 2F), may indicate a defect in sister-chromatid association in *Rec8*$^{-/-}$ spermatocytes.

We next examined whether RAD21/SCC1, the paralog of *Rec8*, was present on chromosomes in *Rec8*$^{-/-}$ spermatocytes. RAD21/SCC1 was recently shown to localize along meiotic chromosome arms and around the centromeres in both male and female mouse meiocytes (Parra et al., 2004; Prieto et al., 2002; Prieto et al., 2004; Xu et al., 2004). The chromosomal distribution of RAD21/SCC1 in *Rec8*$^{-/-}$ leptotene-like nuclei was similar to that of wt (data not shown). RAD21/SCC1 was clearly evident on chromosomal axes of both wt pachytene (Figure 4D) and *Rec8*$^{-/-}$ zygotene-like (Figure 4E) spermatocytes, in an essentially contiguous fashion. Similarly, binding of RAD21/SCC1 to the centromeric region appeared to be retained in *Rec8*$^{-/-}$ spermatocytes (Figures 4F and 4G). Collectively, these data demonstrate that other cohesin subunits are capable of binding to chromosomal cores and centromeric regions in the absence of REC8.

RAD51/DMC1 Foci Are Formed and Resolved on *Rec8* Null Univalents

In wt mice, RAD51/DMC1-containing complexes appear as multiple foci along the axes of unsynapsed chromosomes at the site of SPO11-induced DNA DSBs (Figure 5A); their numbers decrease following synapsis such that they have almost disappeared (except on XY chromosomes) by late pachytene (Figures 5B and 5C). Their resolution is complete before entry into metaphase I (Barlow et al., 1997; Moens et al., 2002).

Large numbers of RAD51/DMC1 foci were visualized along the SCP3-labeled axes of unsynapsed sister chromatids in *Rec8*$^{-/-}$ leptotene (data not shown) and early zygotene-like (type A) spermatocytes (Figure 5D), suggesting that DNA DSBs were produced with appropriate timing for the initiation of recombination. The numbers of RAD51/DMC1 foci were low in the majority of *Rec8*$^{-/-}$ zygotene-like nuclei (Figures 5E and 5F). This observation differs from that reported for the *mei8* mutant, which had no apparent reduction in the number of RAD51/DMC1 foci (Bannister et al., 2004). It is possible that this difference could be due to residual activity of the REC8 N-terminal domain in the *mei8* mutant. Alternatively, variation in the number of cells examined between the two studies might account for this difference, as we noted that a subset of *Rec8*$^{-/-}$ zygotene-like cells (type C) had clusters of RAD51/DMC1 foci in the vicinity of AE breaks (data not shown).

We next examined whether these early recombination events led to the development of reciprocal exchanges (crossovers) between homologous chromosomes in *Rec8*$^{-/-}$ cells. Crossover events cannot be directly visualized, but structures such as late recombination nodules and chiasmata occur at, and are markers for, crossover sites (Pittman and Schimenti, 1998). Likewise, MLH1, a eukaryotic ortholog of the bacterial *MutL* mismatch repair protein, is known to associate with crossover sites (Anderson et al., 1999). While at least one MLH1 focus per chromosome was observed in wt pachytene spermatocytes (Figure 5G), MLH1 foci

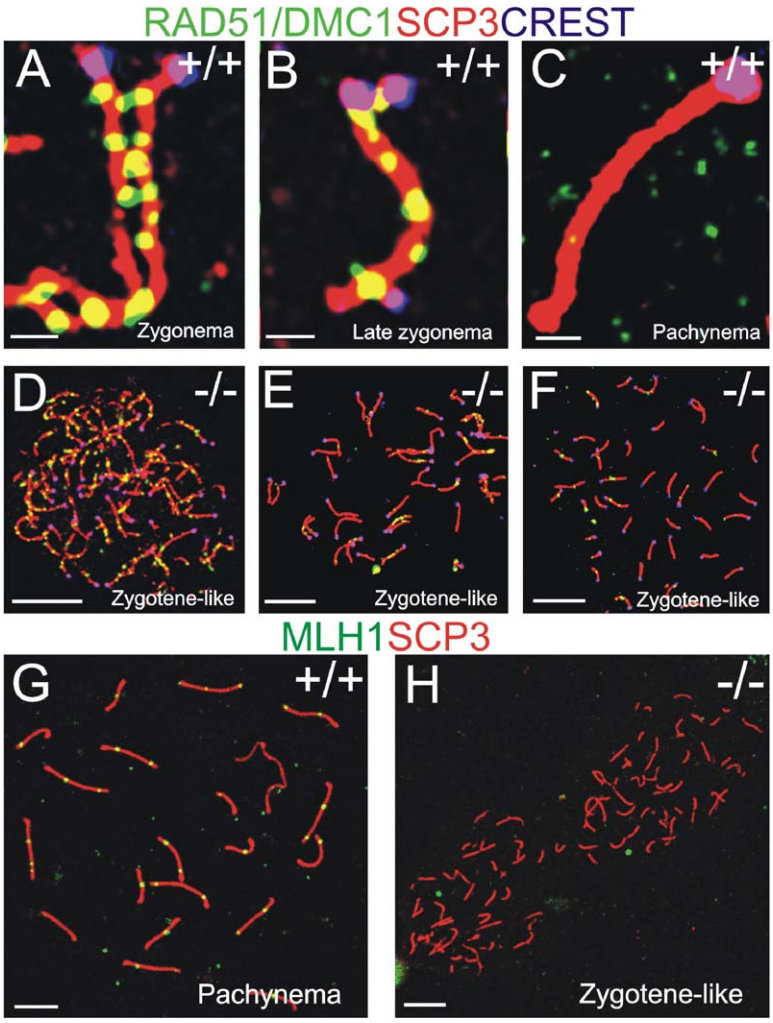

Figure 5. Analysis of RAD51/DMC1 and MLH1 Staining on Wild-Type and *Rec8*$^{-/-}$ Meiotic Chromosome Cores

(A–C) Progressive loss of RAD51/DMC1 foci through prophase I in wt spermatocytes. RAD51/DMC1 foci (yellow-green) demarcate meiotic DNA DSBs; here the chromosome axes are costained with SCP3 (red) and CREST (centromeres: purple).

(D–F) *Rec8*$^{-/-}$ nuclei shown are (D) zygotene-like type A with many RAD51/DMC1 foci; (E) zygotene-like, with paired and partially conjoined chromosomes and few RAD51/DMC1 foci; (F) zygotene-like, with 40 dispersed chromosomes and infrequent RAD51/DMC1 foci.

(G) Wild-type pachytene cells. One or two yellow dots, representing MLH1 foci (yellow, thought to mark crossover sites) were evident on each chromosome, the cores of which are costained with SCP3 (red).

(H) Two *Rec8*$^{-/-}$ zygotene-like nuclei. No MLH1 foci are present on mutant chromosomes of any configuration.

Scale bars equal 1 μM in (A)–(C) and 10 μM in (D)–(H).

were totally absent from *Rec8*$^{-/-}$ spermatocyte chromosomes (Figure 5H).

Female *Rec8* Null Mice Have Germ Cell Failure, Sterility, and Meiotic Sister Synapsis

Several mammalian meiotic mutants display phenotypic sexual dimorphism. For example, spermatogenesis arrests in pachytene in both *SMC1β*$^{-/-}$ and *SCP3*$^{-/-}$ mutants, whereas oogenesis proceeds to metaphase II in *SMC1β*$^{-/-}$ females, and *SCP3*$^{-/-}$ females are fertile (Revenkova et al., 2004; Yuan et al., 2000). Accordingly, we examined *Rec8*$^{-/-}$ females to determine if the defects observed in *Rec8*$^{-/-}$ spermatocytes occurred also during oogenesis. In mice, female germ cells enter into meiosis during embryogenesis with the appearance of leptotene cells at 13.5 days postcoitum (dpc), zygotene and pachytene cells between 15.5 dpc and 18.5 dpc, and diplotene cells at birth (McClellan et al., 2003).

Like males, *Rec8*$^{-/-}$ female mice were sterile. Histological examination of ovaries from 18.5 dpc *Rec8*$^{-/-}$ females revealed that prophase I germ cells were indeed present but that abnormal germ cells with highly compacted chromosomes (compared to wt oocytes) could be discerned (Figures 6A–6D). *Rec8*$^{-/-}$ day 5 neonatal ovaries (and later days up to adult ovaries; data not shown) were characterized by a complete absence of oocytes and ovarian follicles and a dense fibrovascular stoma (Figures 6E–6H). Additionally, the genital tract of *Rec8*$^{-/-}$ females was involuted, probably as an indirect consequence of ovarian hormonal failure, secondary to the lack of follicles (data not shown).

SCP3 immunofluorescent staining of chromosome spreads from oocytes of 16.5 to 18.5 dpc showed the presence of typical leptotene chromosomes in both wt and *Rec8*$^{-/-}$ ovaries (Supplemental Table S3). Pachytene nuclei, with their characteristic 20 pairs of synapsed homologous chromosomes, were clearly evident in wt oocytes (Figure 6I). Zygotene-like chromosome configurations were observed in *Rec8*$^{-/-}$ oocytes (Figure 6J and Supplemental Table S3), but typical pachytene oocytes were absent in *Rec8*$^{-/-}$ ovaries. As with *Rec8*$^{-/-}$ spermatocytes, homolog synapsis was defective, as evident from the presence of ~40 chromosome cores in some *Rec8*$^{-/-}$ oocyte spreads (Figure 6J). That this appearance simply represented chromosome fragmentation was excluded, based on the pres-

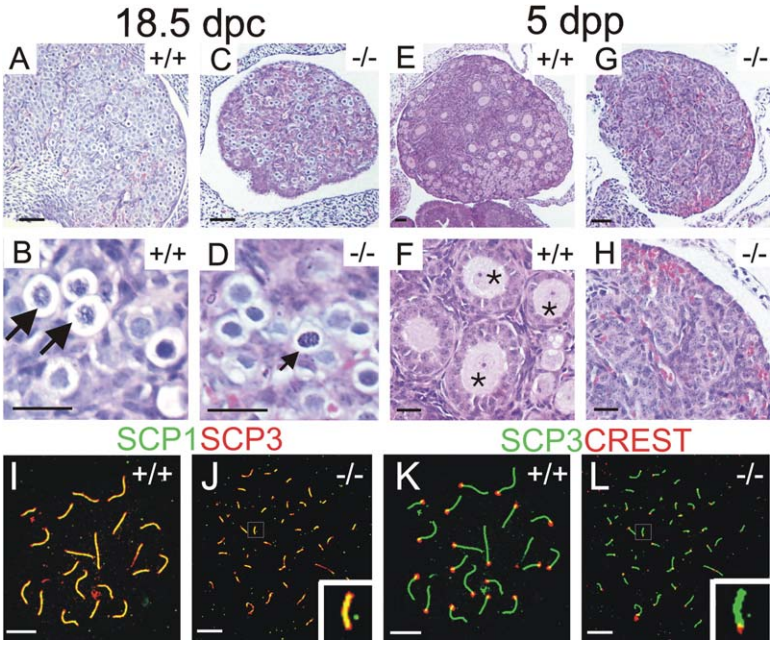

Figure 6. Failure of Oogenesis in *Rec8*$^{-/-}$ Mice

(A–D) H&E staining of ovarian sections of prenatal wt and *Rec8*$^{-/-}$ littermates at 18.5 dpc. Germ cells (arrows) are evident in both wt (A and B) and *Rec8*$^{-/-}$ (C and D) littermates. dpc, days postcoitus.

(E–H) H&E staining of ovarian sections of postnatal wt and *Rec8*$^{-/-}$ littermates at 5 dpp. Mature ovarian follicles and oocytes (asterisks) are evident in wt animals (E and F), but no follicles or oocytes were observed in *Rec8*-null littermates (G and H). dpp, days postpartum.

(I–L) Immunostaining of chromosome spreads of pachytene oocytes from wt (I and K) and zygotene-like oocytes from *Rec8*$^{-/-}$ (J and L) littermates at 17.5 dpc. Labeling proteins and colors are depicted across the top of the panels. Colocalization: yellow. 20 fully synapsed wt homologous chromosomes are indicated by costaining of SCP3 and SCP1 (I) with centromeres marked by costaining with CREST (K). SCP1 coats the majority of the univalents in *Rec8*$^{-/-}$ oocytes (J). CREST staining (L) shows that the great majority of the chromosome cores in this oocyte have centromeres.

Scale bars equal 40 μM in (A), (C), (E), and (G), 20 μM in (B), (D), (F), and (H), and 10 μM in (I)–(L).

ence of CREST-positive centromeres on essentially all univalents (Figures 6K and 6L for wt and *Rec8*$^{-/-}$, respectively). Further, SCP1 coated individual univalents in oocytes, indicating that the SC mislocalization phenotype was sexual monomorphic (i.e., as also seen in spermatocytes) (Figure 6J). As was observed in males, the apparent loss of association between sister chromatids that is accompanied by chromosome fragmentation was evident in some *Rec8*$^{-/-}$ zygotene-like (type C) oocyte nuclei (Supplemental Table S3).

Discussion

We report here that in both males and females, the *Rec8*$^{-/-}$ meiotic phenotype is one of a prophase I arrest, with the novel feature of sister-chromatid synapsis. Since the initial chromosome partner search and homolog alignment is apparently intact in *Rec8*$^{-/-}$ meiocytes, the role of REC8 is likely to be limited to the subsequent intimate chromosome associations of synapsis.

REC8 Is Required for Prevention of SC Formation between Sister Chromatids

Defects in the early stages of meiotic chromosome synapsis have been reported in several mouse mutants, including *Spo11*$^{-/-}$, *Dmc1*$^{-/-}$, *Hop2*$^{-/-}$, and *Fkbp6*$^{-/-}$ (Baudat et al., 2000; Crackower et al., 2003; Petukhova et al., 2003; Pittman et al., 1998). However, notable differences exist between the *Rec8*$^{-/-}$ mutant phenotypes reported here and those mutants previously described. In *Spo11*, *Dmc1*, *Hop2*, and *Fkbp6* null spermatocytes, synapsis typically occurs between nonhomologous (i.e., different) chromosomes (Baudat et al., 2000; Crackower et al., 2003; Petukhova et al., 2003; Pittman et al., 1998). In contrast, in *Rec8*$^{-/-}$ cells, nonhomologous synapsis was not observed. Instead, in meiocytes from both male and female *Rec8*$^{-/-}$ animals, an SC-like structure comprising two AE/LEs and a CE was present between sister chromatids, rather than between homologous chromosomes (Figure 7). The *Rec8*$^{-/-}$ cell has an inability to discern sister chromatids from homologous chromosomes, suggesting that REC8 might either enforce a close physical association of sister chromatids, or limit the potential SC binding sites of each sister chromatid, such that effectively, only one chromosome surface is available for loading and attachment of synaptic components onto a given univalent (sister-chromatid pair). Under normal circumstances, this should restrict SC formation to between homologous chromosomes (Figure 7A). In the absence of REC8, the tight association of sister chromatids might be perturbed, although sister chromatids may be kept in general proximity by a non-REC8-containing cohesin complex or other unknown mechanisms. Potential binding sites for the main SC components on each sister chromatid may become accessible, thereby allowing the formation of SC between sister chromatids (Figure 7B). The observation that any homologous synapsis was rare in *Rec8*$^{-/-}$ meiocytes suggests that sister chromatids in such an instance became a preferred site for binding of the main SC components. This proposition is consistent with genetic studies in budding yeast that suggest that a REC8-related event in S phase has an important role in the subsequent coordination of interhomolog and intersister interactions (Cha et al., 2000).

Alternatively, a REC8-containing cohesin complex might physically occlude potential SC binding site(s) on a sister chromatid, although this implies an asymmetry

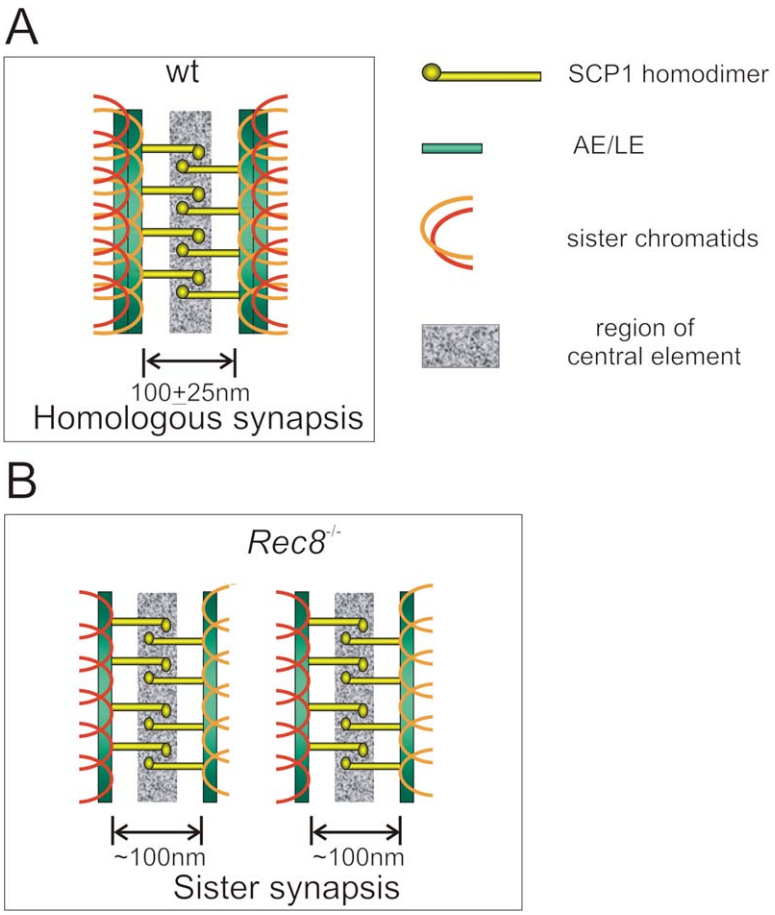

Figure 7. Diagram Illustrating Effects of REC8 Loss on SC Formation

(A) In wt cells, the SC forms between homologous chromosomes ("homologous synapsis"). The mature SC has a tripartite structure on EM (two lateral elements [LE] and a central element [CE]; also see Figure 3J). Two individual sister chromatids (red and orange) are in close proximity. SCP1 homodimers (yellow) bind the LEs (green bars) of homologous chromosomes and transfix them in a zipper-like fashion, thereby forming SCs. The SCP1 homodimers interact medially via their globular head domains, contributing to the CE (gray area) of the SC. SC dimensions measured from sectioned or surface-spread chromosomes by EM have a total width of about 194 ± 13 nm with a central region of 100 ± 25 nm (Dobson et al., 1994).
(B) In *Rec8*$^{-/-}$ cells, SC form between sister chromatids ("sister synapsis"). SCP1 polymerizes onto AEs/LEs associated with only a single sister chromatid, again strutting apart the cores by a distance similar to the LE separation between homologous chromosomes in wt cells (also see Figures 3J–3M).

of the complex that is established during DNA replication along one sister chromatid but not the other. We favor the former explanation of REC8's involvement in synapsis in which binding sites for SC filaments exist along both sister chromatids, but in the normal case are prevented by REC8 from interacting with each other and are thus available for pairing only with a homologous chromosome.

Sister-Chromatid Cohesion in *Rec8*$^{-/-}$ Germ Cells

REC8 serves disparate roles in regulating meiotic chromosome behavior in different species. In budding yeast, REC8 is essential for SCC both along chromosome arms and on centromeres (Klein et al., 1999), whereas in fission yeast, deletion of *Rec8* compromises only arm cohesion and SCC is maintained at centromeres in meiosis I (Kitajima et al., 2003; Molnar et al., 1995; Watanabe and Nurse, 1999). Whether SCC is established and maintained in the absence of mouse REC8 is currently unknown. In both budding and fission yeasts, the REC8 paralog, RAD21/SCC1, can functionally substitute for REC8 in supporting meiotic SCC when expressed ectopically in the absence of REC8 (Toth et al., 2000; Yokobayashi et al., 2003). Mammalian RAD21/SCC1 coexists with REC8 on meiotic chromosome cores, both along arms and at centromeres, and its distribution was topologically and temporally consistent with its participation in meiotic SCC (Parra et al., 2004; Prieto et al., 2004; Xu et al., 2004). The chromosomal distribution and behavior of RAD21/SCC1 in these studies thus led to the suggestion that it may contribute to meiotic SCC, although this function in mammalian meiosis is yet to be established. We observed that RAD21/SCC1 and SMC3 cohesin were present along chromosome arms and on centromeres in *Rec8*$^{-/-}$ spermatocytes. This raises the possibility that a RAD21/SCC1-containing complex may provide SCC in *Rec8*$^{-/-}$ meiocytes. However, it has been proposed that in mitotic cells at least, cohesin forms a proteinaceous ring of diameter ~45 nm encircling sister chromatids, with the V-shaped SMC heterodimers interconnected by RAD21/SCC1 subunit in a "hairclip" fashion (Gruber et al., 2003; Haering et al., 2002; Haering et al., 2004). The SC-like structure that assembles between sister chromatids of *Rec8* null spermatocyte chromosomes is ultrastructurally indistinguishable from the wt SC (Figures 3J–3M). SC dimensions, measured from electron micrographs of sectioned or surface-spread chromosomes, was reported by Dobson et al. (1994) to have a total width of about 194 ± 13 nm with an internal diameter of 100 ± 25 nm (also see Figure 7A). Given that the width of the SC is approximately 4-fold the predicted diameter of the cohesin ring, it is difficult to envisage that the formation of an SC-like structure that spans approximately 100 nm between sister chroma-

tids in *Rec8*$^{-/-}$ meiocytes could take place in the presence of SCC maintained by a RAD21/SCC1-containing complex. We cannot, however, presently exclude the possibility that other conformations exist for a RAD21/SCC1-containing cohesin complex. Nevertheless, sister chromatids appeared to remain in the proximity of each other in the majority of *Rec8*$^{-/-}$ meiocytes, as apparent separation of sister chromatids was observed in only a subset of *Rec8*$^{-/-}$ meiocytes. A RAD21/SCC1-containing cohesin complex could possibly assist in maintaining sister chromatids in the proximity of each other, either in a temporal fashion or by interlinking loops of DNA. Additionally, the SC-like structure forming aberrantly between sister chromatids may act as a surrogate form of cohesin and bind together sister chromatids. It is currently not possible to differentiate between these possibilities. Functional studies of mammalian meiotic mutants, which either selectively abrogate RAD21/SCC1 function in meiotic cells or prevent the formation of the SC-like structure between sister chromatids in *Rec8*$^{-/-}$ cells, would be helpful in resolving these issues.

A Role for Mouse REC8 in DSB Repair and Homologous Recombination

Absence of REC8 leads to hyperresection of DNA DSBs in budding yeast (Klein et al., 1999) and reduced (region-specific) recombination in fission yeast (Parisi et al., 1999). During normal meiotic progression, homologous recombination commences with the formation of SPO11-induced DNA DSBs (Pittman and Schimenti, 1998). After exonuclease resection of DSB ends, RAD51/DMC1 recombinase binds to the DSB sites, early recombination nodules form, and most DSBs are repaired by homologous recombination. Late recombination nodule represents retained crossover sites.

Our data showed that RAD51/DMC1 foci were present along the axes of *Rec8*$^{-/-}$ chromosomes, suggesting that early recombination events, including the genesis of DNA DSBs and binding of RAD51/DMC1 to DSBs following strand resection, occur in *Rec8*$^{-/-}$ spermatocytes (Gasior et al., 2001). Subsequent disappearance of RAD51/DMC1 foci indicated that at least grossly, the initial repair of axial DSBs occurred in the absence of REC8. MLH1 foci, which localize to late recombination nodules in late pachytene (Moens et al., 2002) and mark crossovers (Anderson et al., 1999), were not detected in *Rec8*$^{-/-}$ cells, including those with partial bivalent synapsis. The absence of MLH1 foci indicates that the processes of homologous recombination are disrupted in the absence of REC8, despite indirect evidence for the formation of early recombination intermediates. Although this could reflect a direct or indirect role for REC8 in DSB repair, the most parsimonious explanation may be that *Rec8*$^{-/-}$ cells do not reach the stage of late recombination nodule formation before being eliminated. Alternatively, crossovers in *Rec8*$^{-/-}$ cells might occur, but without the assembly of normal late MLH1-positive recombination nodules.

Disruption in homologous recombination in *Rec8*$^{-/-}$ spermatocytes could result from defects in homolog synapsis, as discussed above. Defects in DSB repair may be an additional factor. We observed that a subset of *Rec8*$^{-/-}$ spermatocytes had numerous RAD51/DMC1 foci along the chromosome axes. The persistence of RAD51/DMC1 foci in these cells may reflect inability of *Rec8*$^{-/-}$ spermatocytes to effectively repair DSBs. Further, the loss of oocytes during early stages of meiosis and the lack of follicle formation in *Rec8*$^{-/-}$ females resemble the phenotypes of DSB repair-defective mutants (i.e., *Dmc1*$^{-/-}$) but are distinct from that of DSB formation-defective mutants such as *Spo11*$^{-/-}$ (Di Giacomo et al., 2005). This observation, although circumstantial, is evidence for a DSB repair defect in *Rec8*$^{-/-}$ meiocytes.

Mammalian REC8

Disruption of REC8 function in budding and fission yeast and *C. elegans* resulted in a failure of SC formation (Klein et al., 1999; Molnar et al., 1995; Watanabe and Nurse, 1999). We showed that the formation of SC-like structures occur in the absence of REC8 in mice, but in an aberrant location, namely, between sister chromatids. As a result of our analysis, we propose that the presence of mammalian REC8 on axial cores of meiotic chromosomes is essential for cells to make the critical distinction between sister chromatids and homologous chromosomes. A potential role for involvement of mammalian REC8 in regulating chromosome segregation through meiosis I and II, as shown in a number of studies on other species, was unable to be examined in this study, due to the prophase I loss of *Rec8*$^{-/-}$ meiocytes. Strategies such as in vitro differentiation (Feng et al., 2002) of *Rec8 null* spermatogonial stem cells expressing partial functional or conditional *Rec8* alleles might be used to explore this possibility.

It is interesting to note that the *Rec8* null mutant had a grossly similar phenotype of synaptic failure to the *mei8* mutant, which would be predicted to potentially retain the conserved REC8 N-terminal domain (Bannister et al., 2004). Since REC8 protein was not detected on meiotic pachytene chromosomes in the *mei8* males (Bannister et al., 2004), a possible explanation is that truncated REC8 may not correctly associate with the cohesin complex in the *mei8* mutant, resulting in phenotypes similar to the *Rec8*-null mutant. Studies of yeast cohesin complex architecture revealed that binding of the C-terminal domain of RAD21/SCC1 to SMC1 is a prerequisite for the binding of the N-terminal domain to SMC3 and probably for the formation of a functional cohesin complex (Arumugam et al., 2003; Haering et al., 2004). Strong conservation between the N- and C-terminal domains of REC8 and RAD21/SCC1 kleisins suggests that these domains in REC8 may interact with SMCs in a similar fashion (Arumugam et al., 2003; Haering et al., 2004; Schleiffer et al., 2003).

The high mortality rate and the reduced growth seen in *Rec8*$^{-/-}$ animals (this study) were not described in the *mei8* mutant (Bannister et al., 2004). It is possible that the manipulation of the *Rec8* allele may affect the function of an unrelated gene(s), being thus responsible for the somatic phenotypes. We cannot rule out the possibility that mammalian *Rec8* may have a role in one or more nonmeiotic processes during development. Such a somatic function for REC8 may not require assembly of the cohesin complex, but rather, may be a

new developmental function acquired (possibly by the N-terminal domain) by REC8 during the evolution of mammals. Further experiments are required to determine the nature of the somatic defects of *Rec8*$^{-/-}$ animals.

Experimental Procedures

Cloning the *Rec8* cDNA and Genomic Locus

The *Rec8* cDNA was cloned by searching the EST database for a mouse EST homologous to the human REC8 (*hrec8*) sequence. One EST (AA050562) had significant similarity to the central and 3′ regions of the *hrec8* gene. The 5′ sequence was obtained by 5′ RACE using RNA isolated from mouse testis. The *Rec8* cDNA sequence (GenBank accession AF262055) was assembled and then used to screen a 129/SvJ mouse genomic library from which clones were obtained. The exon/intron structure of the *Rec8* gene was determined through comparison of the genomic sequence with that of the cDNA.

Targeted Disruption of the *Rec8* Gene

Mouse Genome Sequence Database revealed two chromosomal loci having homology to *Rad21* (http://www.ncbi.nlm.nih.gov/genome/seq/MmHome.html). These include the *Rec8* ortholog on chromosome 14 and a *Rad21*-like gene on chromosome 15. Targeting arms of 1.4 kb and 5.5 kb, 5′ and 3′ to the *Rec8* gene, respectively, were PCR generated from W9.5 ES cell line genomic DNA and directionally cloned flanking a pgk-Neo cassette, obtained from the pPNT vector. A GFP cassette was introduced in-frame with the *Rec8* promoter sequence upstream from the neomycin resistance cassette, at the start site of translation of the endogenous *Rec8* gene. Expression from this reporter was not detected in either heterozygous or homozygous *Rec8* KO mice. A pgk-TK cassette, also from pPNT, was inserted for negative selection against random integrants.

Linearized *Rec8* targeting construct was electroporated into W9.5 ES cells. After culture for 5 days in media supplemented with 200 μg/ml G418 and 2 μM gancyclovir, drug-resistant clones were screened for homologous recombination with the *Rec8* locus by Southern blotting of *Eco*RI-digested genomic DNA with a 0.5 kb external probe 3′ to the *Rec8* gene. Targeted clones were microinjected into C57BL/6 blastocysts. One *Rec8*-targeted clone produced highly chimeric males that were crossed to C57BL/6 or 129/SvJ females. Germline transmission of the *Rec8* null allele was confirmed by PCR analysis of tail DNA from F1 offspring. Heterozygous *Rec8* KO mice were interbred to homozygosity. The phenotypes of *Rec8*$^{-/-}$ mice on both genetic backgrounds were identical. The selection cassettes at the targeted locus were removed by intercrossing with CMV-*Cre* mice.

Rec8 expression in the testis of wild-type and knockout animals was evaluated by Northern. A 5′ fragment of *Rec8* cDNA (nucleotides 278–961) was hybridized to a Northern blot loaded with 10 μg of total mouse testis RNA from each *Rec8* genotype.

Histological Analysis

Tissues were fixed in 10% buffered formalin for 2–4 hr before being dehydrated, embedded in paraffin wax, and sectioned. Sections were stained with hematoxylin and eosin. For detection of apoptotic cells within the testes, TUNEL staining was performed as previously described (Ansari et al., 1993). Immunohistochemistry was performed with mouse monoclonal anti-PCNA (DAKO) at dilution of 1:1000 using a TSA kit (DAKO) according to the manufacturer's instructions. Sections were counterstained with hematoxylin.

Silver Staining and EM Analysis of SC

Spermatocyte chromosomes were surface spread, as described above, and stained using a 50% (w/v) solution of silver nitrate at 55°C for 12–18 hr or until slides became light brown. For EM ultrastructure analysis, chromosome spreads were prepared on slides coated with 0.5% Formvar (Pro Sci Tech, Australia) and stained as described above. The film containing the spreads was transferred to 50 mesh hexagonal nickel grids. Grids were viewed with a Hitachi H-600 Electron Microscope.

Immunofluorescence of Surface-Spread Spermatocyte Chromosomes

Chromosome spreads of spermatocytes and oocytes were prepared using a dry-down method (Peters et al., 1997). Primary antibodies used were rabbit anti-SCP3 (gift from C. Heyting), goat anti-SCP3 (gift from T. Ashley), mouse polyclonal anti-SYN1/SCP1 (gift from P. Moens), rabbit anti-SMC3 (gift from R. Jessberger), rabbit anti-RAD51 (H-92) (Santa Cruz), CREST-6 (gift from A. Choo), affinity-purified rabbit anti-human RAD21/SCC1 (gift from J.M. Peters), and monoclonal anti-MLH1 (Santa Cruz). Secondary antibodies were Alexa 488 donkey anti-sheep IgG, Alexa 488 goat anti-rabbit IgG, Alexa 568 goat anti-mouse IgG, and Alexa 647 goat anti-human IgG (Molecular Probes). DNA was stained with DAPI (4',6'-diamidino-2-phenylindole). Data collection was on either a Zeiss Axioskop 2 microscope or confocal microscope (Bio Rad MRC 1000). Images were manipulated using Confocal Assistant 4.02 and Adobe Photoshop software.

Chromosome Painting and Immunostaining of Surface-Spread Spermatocyte Chromosomes

Spermatocyte chromosome spreads and SCP3 immunostaining were performed as described above. Spreads were then fixed in 4% paraformaldehyde and dehydrated through ethanol. For chromosome painting, slides were denatured in 50% formamide, 6x SSC (1x SSC containing 0.15 M NaCl and 0.015 M sodium citrate) at 80°C for 10 min. Hybridization was conducted using biotin-labeled mouse chromosome 10 paint probe (ID Labs, Canada) at 37°C for 72 hr. Signal was detected using a TSA Alexa 488 streptoavidin kit (Molecular Probes). Of 48 *Rec8*$^{-/-}$ spermatocytes examined, 17 cells (35%) had a clear FISH signal. Of these 17 cells, two distantly paired axes were seen embedded in the chromosome 10 FISH signal in all *Rec8*$^{-/-}$ cells. The remaining 31 cells were unable to be scored due to high background.

Supplemental Data

Supplemental Data include four figures and three tables and can be found with this article online at http://www.developmentalcell.com/cgi/content/full/8/6/949/DC1/.

Acknowledgments

The authors thank Sandra Verschoor and Caroline Farrelly for technical assistance; Ralph Rossi for assistance with cell sorting; Paul Waring for histological evaluation of mice; Olivia Cakebread for animal keeping; Sara Ellis for helping with microscopy; and Drs. Kate Loveland, Jeff Craig, Jan Hoeijmakers, Carl Sprung, and Patrick Humbert for comments on the manuscript. We are particularly grateful to Dr. Nobuaki Kudo for kind advice on IF/FISH and for critical reading of the manuscript. We also thank Drs. Terry Ashley, Andy Choo, Christa Heyting, Rolf Jessberger, Peter Moens, Jan-Michael Peters, and Barbara Spyropoulos for gifts of antibodies. Work in the M.J.M. laboratory is supported by the Australian National Health and Medical Research Council, Project Grant numbers 9936643 and 251686.

Received: December 13, 2004
Revised: January 25, 2005
Accepted: March 30, 2005
Published: June 6, 2005

References

Anderson, L.K., Reeves, A., Webb, L.M., and Ashley, T. (1999). Distribution of crossing over on mouse synaptonemal complexes using immunofluorescent localization of MLH1 protein. Genetics *151*, 1569–1579.

Ansari, B., Coates, P.J., Greenstein, B.D., and Hall, P.A. (1993).

In situ end-labelling detects DNA strand breaks in apoptosis and other physiological and pathological states. J. Pathol. *170*, 1–8.

Arumugam, P., Gruber, S., Tanaka, K., Haering, C.H., Mechtler, K., and Nasmyth, K. (2003). ATP hydrolysis is required for cohesin's association with chromosomes. Curr. Biol. *13*, 1941–1953.

Bannister, L.A., Reinholdt, L.G., Munroe, R.J., and Schimenti, J.C. (2004). Positional cloning and characterization of mouse mei8, a disrupted allelle of the meiotic cohesin Rec8. Genesis *40*, 184–194.

Barlow, A.L., Benson, F.E., West, S.C., and Hulten, M.A. (1997). Distribution of the Rad51 recombinase in human and mouse spermatocytes. EMBO J. *16*, 5207–5215.

Baudat, F., Manova, K., Yuen, J.P., Jasin, M., and Keeney, S. (2000). Chromosome synapsis defects and sexually dimorphic meiotic progression in mice lacking Spo11. Mol. Cell *6*, 989–998.

Beasley, M., Warren, W., Hoeijmakes, J., van der Horst, B., and McKay, M.J. (1999). Mammalian mutants of the mrec8 homologous recombination gene: components of a conserved gene family implicated in the DNA damage response, genome stabilisation and chromosome cohesion. In Radiation Research Vol. 2, Proceedings of the 11th ICRR, M. Moriaty, C. Mothersill, C. Seymour, M. Edington, J.F. Ward, and R.J.M. Fry, eds., pp. 593–597.

Cha, R.S., Weiner, B.M., Keeney, S., Dekker, J., and Kleckner, N. (2000). Progression of meiotic DNA replication is modulated by interchromosomal interaction proteins, negatively by Spo11p and positively by Rec8p. Genes Dev. *14*, 493–503.

Chan, R.C., Chan, A., Jeon, M., Wu, T.F., Pasqualone, D., Rougvie, A.E., and Meyer, B.J. (2003). Chromosome cohesion is regulated by a clock gene paralogue TIM-1. Nature *423*, 1002–1009.

Ciosk, R., Shirayama, M., Shevchenko, A., Tanaka, T., Toth, A., and Nasmyth, K. (2000). Cohesin's binding to chromosomes depends on a separate complex consisting of Scc2 and Scc4 proteins. Mol. Cell *5*, 243–254.

Crackower, M.A., Kolas, N.K., Noguchi, J., Sarao, R., Kikuchi, K., Kaneko, H., Kobayashi, E., Kawai, Y., Kozieradzki, I., Landers, R., et al. (2003). Essential role of Fkbp6 in male fertility and homologous chromosome pairing in meiosis. Science *300*, 1291–1295.

Di Giacomo, M., Barchi, M., Baudat, F., Edelmann, W., Keeney, S., and Jasin, M. (2005). Distinct DNA-damage-dependent and -independent responses drive the loss of oocytes in recombination-defective mouse mutants. Proc. Natl. Acad. Sci. USA *102*, 737–742.

Dietrich, A.J., van Marle, J., Heyting, C., and Vink, A.C. (1992). Ultrastructural evidence for a triple structure of the lateral element of the synaptonemal complex. J. Struct. Biol. *109*, 196–200.

Dobson, M.J., Pearlman, R.E., Karaiskakis, A., Spyropoulos, B., and Moens, P.B. (1994). Synaptonemal complex proteins: occurrence, epitope mapping and chromosome disjunction. J. Cell Sci. *107*, 2749–2760.

Eijpe, M., Heyting, C., Gross, B., and Jessberger, R. (2000). Association of mammalian SMC1 and SMC3 proteins with meiotic chromosomes and synaptonemal complexes. J. Cell Sci. *113*, 673–682.

Eijpe, M., Offenberg, H., Jessberger, R., Revenkova, E., and Heyting, C. (2003). Meiotic cohesin REC8 marks the axial elements of rat synaptonemal complexes before cohesins SMC1{beta} and SMC3. J. Cell Biol. *160*, 657–670.

Feng, L.X., Chen, Y., Dettin, L., Pera, R.A., Herr, J.C., Goldberg, E., and Dym, M. (2002). Generation and in vitro differentiation of a spermatogonial cell line. Science *297*, 392–395.

Gasior, S.L., Olivares, H., Ear, U., Hari, D.M., Weichselbaum, R., and Bishop, D.K. (2001). Assembly of RecA-like recombinases: distinct roles for mediator proteins in mitosis and meiosis. Proc. Natl. Acad. Sci. USA *98*, 8411–8418.

Gruber, S., Haering, C.H., and Nasmyth, K. (2003). Chromosomal cohesin forms a ring. Cell *112*, 765–777.

Guacci, V., Koshland, D., and Strunnikov, A. (1997). A direct link between sister chromatid cohesion and chromosome condensation revealed through the analysis of MCD1 in *S. cerevisiae*. Cell *91*, 47–57.

Haering, C.H., Lowe, J., Hochwagen, A., and Nasmyth, K. (2002). Molecular architecture of SMC proteins and the yeast cohesin complex. Mol. Cell *9*, 773–788.

Haering, C.H., Schoffnegger, D., Nishino, T., Helmhart, W., Nasmyth, K., and Lowe, J. (2004). Structure and stability of cohesin's Smc1-kleisin interaction. Mol. Cell *15*, 951–964.

Hartman, T., Stead, K., Koshland, D., and Guacci, V. (2000). Pds5p is an essential chromosomal protein required for both sister chromatid cohesion and condensation in *Saccharomyces cerevisiae*. J. Cell Biol. *151*, 613–626.

Jessberger, R. (2002). The many functions of SMC proteins in chromosome dynamics. Nat. Rev. Mol. Cell Biol. *3*, 767–778.

Kitajima, T.S., Yokobayashi, S., Yamamoto, M., and Watanabe, Y. (2003). Distinct cohesin complexes organize meiotic chromosome domains. Science *300*, 1152–1155.

Klein, F., Mahr, P., Galova, M., Buonomo, S.B., Michaelis, C., Nairz, K., and Nasmyth, K. (1999). A central role for cohesins in sister chromatid cohesion, formation of axial elements, and recombination during yeast meiosis. Cell *98*, 91–103.

Lammers, J.H., Offenberg, H.H., van Aalderen, M., Vink, A.C., Dietrich, A.J., and Heyting, C. (1994). The gene encoding a major component of the lateral elements of synaptonemal complexes of the rat is related to X-linked lymphocyte-regulated genes. Mol. Cell. Biol. *14*, 1137–1146.

Lee, J., Iwai, T., Yokota, T., and Yamashita, M. (2003). Temporally and spatially selective loss of Rec8 protein from meiotic chromosomes during mammalian meiosis. J. Cell Sci. *116*, 2781–2790.

McClellan, K.A., Gosden, R., and Taketo, T. (2003). Continuous loss of oocytes throughout meiotic prophase in the normal mouse ovary. Dev. Biol. *258*, 334–348.

McKay, M.J., Troelstra, C., van der Spek, P., Kanaar, R., Smit, B., Hagemeijer, A., Bootsma, D., and Hoeijmakers, J.H. (1996). Sequence conservation of the rad21 *Schizosaccharomyces pombe* DNA double-strand break repair gene in human and mouse. Genomics *36*, 305–315.

Meuwissen, R.L., Offenberg, H.H., Dietrich, A.J., Riesewijk, A., van Iersel, M., and Heyting, C. (1992). A coiled-coil related protein specific for synapsed regions of meiotic prophase chromosomes. EMBO J. *11*, 5091–5100.

Michaelis, C., Ciosk, R., and Nasmyth, K. (1997). Cohesins: chromosomal proteins that prevent premature separation of sister chromatids. Cell *91*, 35–45.

Moens, P.B., Kolas, N.K., Tarsounas, M., Marcon, E., Cohen, P.E., and Spyropoulos, B. (2002). The time course and chromosomal localization of recombination-related proteins at meiosis in the mouse are compatible with models that can resolve the early DNA-DNA interactions without reciprocal recombination. J. Cell Sci. *115*, 1611–1622.

Molnar, M., Bahler, J., Sipiczki, M., and Kohli, J. (1995). The rec8 gene of *Schizosaccharomyces pombe* is involved in linear element formation, chromosome pairing and sister-chromatid cohesion during meiosis. Genetics *141*, 61–73.

Nasmyth, K. (2001). Disseminating the genome: joining, resolving, and separating sister chromatids during mitosis and meiosis. Annu. Rev. Genet. *35*, 673–745.

Parisi, S., McKay, M.J., Molnar, M., Thompson, M.A., van der Spek, P.J., van Drunen-Schoenmaker, E., Kanaar, R., Lehmann, E., Hoeijmakers, J.H., and Kohli, J. (1999). Rec8p, a meiotic recombination and sister chromatid cohesion phosphoprotein of the Rad21p family conserved from fission yeast to humans. Mol. Cell. Biol. *19*, 3515–3528.

Parra, M.T., Viera, A., Gomez, R., Page, J., Benavente, R., Santos, J.L., Rufas, J.S., and Suja, J.A. (2004). Involvement of the cohesin Rad21 and SCP3 in monopolar attachment of sister kinetochores during mouse meiosis I. J. Cell Sci. *117*, 1221–1234.

Pasierbek, P., Jantsch, M., Melcher, M., Schleiffer, A., Schweizer, D., and Loidl, J. (2001). A *Caenorhabditis elegans* cohesion protein with functions in meiotic chromosome pairing and disjunction. Genes Dev. *15*, 1349–1360.

Peters, A.H., Plug, A.W., van Vugt, M.J., and de Boer, P. (1997). A

drying-down technique for the spreading of mammalian meiocytes from the male and female germline. Chromosome Res. *5*, 66–68.

Petukhova, G.V., Romanienko, P.J., and Camerini-Otero, R.D. (2003). The Hop2 protein has a direct role in promoting interhomolog interactions during mouse meiosis. Dev. Cell *5*, 927–936.

Pittman, D.L., and Schimenti, J.C. (1998). Recombination in the mammalian germ line. Curr. Top. Dev. Biol. *37*, 1–35.

Pittman, D.L., Cobb, J., Schimenti, K.J., Wilson, L.A., Cooper, D.M., Brignull, E., Handel, M.A., and Schimenti, J.C. (1998). Meiotic prophase arrest with failure of chromosome synapsis in mice deficient for Dmc1, a germline-specific RecA homolog. Mol. Cell *1*, 697–705.

Prieto, I., Pezzi, N., Buesa, J.M., Kremer, L., Barthelemy, I., Carreiro, C., Roncal, F., Martinez, A., Gomez, L., Fernandez, R., et al. (2002). STAG2 and Rad21 mammalian mitotic cohesins are implicated in meiosis. EMBO Rep. *3*, 543–550.

Prieto, I., Tease, C., Pezzi, N., Buesa, J.M., Ortega, S., Kremer, L., Martinez, A., Martinez, A.C., Hulten, M.A., and Barbero, J.L. (2004). Cohesin component dynamics during meiotic prophase I in mammalian oocytes. Chromosome Res. *12*, 197–213.

Revenkova, E., Eijpe, M., Heyting, C., Hodges, C.A., Hunt, P.A., Liebe, B., Scherthan, H., and Jessberger, R. (2004). Cohesin SMC1 beta is required for meiotic chromosome dynamics, sister chromatid cohesion and DNA recombination. Nat. Cell Biol. *6*, 555–562.

Schleiffer, A., Kaitna, S., Maurer-Stroh, S., Glotzer, M., Nasmyth, K., and Eisenhaber, F. (2003). Kleisins: a superfamily of bacterial and eukaryotic SMC protein partners. Mol. Cell *11*, 571–575.

Toth, A., Rabitsch, K.P., Galova, M., Schleiffer, A., Buonomo, S.B., and Nasmyth, K. (2000). Functional genomics identifies monopolin: a kinetochore protein required for segregation of homologs during meiosis I. Cell *103*, 1155–1168.

van Heemst, D., James, F., Poggeler, S., Berteaux-Lecellier, V., and Zickler, D. (1999). Spo76p is a conserved chromosome morphogenesis protein that links the mitotic and meiotic programs. Cell *98*, 261–271.

Watanabe, Y., and Nurse, P. (1999). Cohesin Rec8 is required for reductional chromosome segregation at meiosis. Nature *400*, 461–464.

Xu, H., Beasley, M., Verschoor, S., Inselman, A., Handel, M.A., and McKay, M.J. (2004). A new role for the mitotic RAD21/SCC1 cohesin in meiotic chromosome cohesion and segregation in the mouse. EMBO Rep. *5*, 378–384.

Yokobayashi, S., Yamamoto, M., and Watanabe, Y. (2003). Cohesins determine the attachment manner of kinetochores to spindle microtubules at meiosis I in fission yeast. Mol. Cell. Biol. *23*, 3965–3973.

Yuan, L., Liu, J.G., Zhao, J., Brundell, E., Daneholt, B., and Hoog, C. (2000). The murine SCP3 gene is required for synaptonemal complex assembly, chromosome synapsis, and male fertility. Mol. Cell *5*, 73–83.